Green Chemistry

PAPER

View Article Online
View Journal | View Issue

Cite this: *Green Chem.*, 2021, **23**, 6984

Convenient C(sp^3)–H bond functionalisation of light alkanes and other compounds by iron photocatalysis†

Yunhe Jin, *‡ Qingqing Zhang,‡ Lifang Wang, Xinyao Wang, Changgong Meng and Chunying Duan *

Received 5th May 2021,
Accepted 8th July 2021

DOI: 10.1039/d1gc01563j

rsc.li/greenchem

Light alkanes are natural organic carbon sources and widely distributed in nature. Transforming them into value-added fine chemicals affords attractively economic and ecological benefits as well as enormous chemical challenges. Herein, we report a practical iron-catalysed photoredox system for C(sp^3)–H transformation of ethane, propane, and other light alkanes to C–N and C–C bonds under ambient temperature. The present method with abundant and inexpensive iron salts as photocatalysts exhibits high catalytic efficiency (turnover number up to 8000), mild conditions, and the convenience of being purified and scaled up without chromatography. A photo-induced ligand-to-metal charge transfer between Fe(III) and Cl^- generates a highly active chlorine radical that sequentially acts as hydrogen atom transfer catalyst. Therefore, the sustainable, convenient, and environmentally friendly system will find wide applications in high-value-added transformation of natural alkanes with novel inspiration not only for organic synthesis, but also for designing catalytically active organic/inorganic materials.

Introduction

Light alkanes (mainly including C_2–C_6) are widely distributed and abundant in nature, but these organic carbon sources are usually applied as fuels more than as economical chemical feedstocks.[1] The main reason for the case is the great difficulty in direct activation of C(sp^3)–H bonds in light alkanes due to their intrinsic inertness, uncontrollable chemoselectivity, and low solubility in most solvents.[2a] The great scientific challenges and the additional economic and ecological benefits of transforming natural alkanes into value-added liquid fine chemicals by homogeneous catalytic reactions have attracted substantial attention in recent years.[2] To avoid the harsh conditions (high temperature, strong oxidants, and superacid media) used before,[3] noble metal-catalysed (Pd, Ir, Rh, Ru) systems[2d,4] and biomimetic (Fe, Mn, and Co porphyrins) catalytic systems[5] have been developed, but it is a big challenge to exploit efficient catalytic systems without complicated ligands for convenient C(sp^3)–H functionalisation under mild conditions.

Recently, photocatalysis, which is an environmentally friendly, sustainable, and unique process, has received significant attention.[6] Owing to the high activities of radicals, photogenerated oxygen,[7] nitrogen,[8] sulphur[9] and bromine[10] radicals have been enabled to activate unattainable C–H bonds *via* hydrogen atom transfer (HAT) processes. Recently, Zuo,[11a] Wu[11b] and Noël[11c] groups respectively realised direct functionalisation of gaseous alkanes with excellent yields and novel catalytic systems by photo-induced HAT processes; high oxidation potential and high price of the used photocatalysts limit the further development and industrial application of these system to a certain extent. Chlorine radicals are another heteroatom-centred radical capable of processing HAT with unactivated aliphatic C–H bonds,[11b] but little attention has been focused on its application in photocatalysis[12] due to its high oxidation potential ($E^{ox}(Cl^-/Cl^{\bullet})$ = + 2.03 V *vs.* SCE). Photo-dissociation of molecular chlorine in old processes is an effective measure to give chlorine radicals; however, use of toxic, corrosive, and hazardous molecular chlorine affords great application limitation.

Photo-induced ligand-to-metal charge transfers (LMCT), instead of traditional redox processes, seems to be an effective solution to solve this problem.[13] Of all transition metal elements, iron is the most abundant one in the earth's crust, and its low oxidation potential and application in photo-cata-

State Key Laboratory of Fine Chemicals, Zhang Dayu School of Chemistry, Dalian University of Technology, Dalian 116024, China. E-mail: jinyh18@dlut.edu.cn, cyduan@dlut.edu.cn

†Electronic supplementary information (ESI) available: Mechanism investigations, synthetic procedures, characterisation data and ^1H, ^{13}C NMR spectra of these synthesised compounds. See DOI: 10.1039/d1gc01563j

‡These authors contributed equally to this work.

lysed organic synthesis through photo-induced LMCT[5a,14] afford benefits to overcome this key challenge. From the perspective of sustainability, we hope to employ the chlorine radicals generated from photo-induced LMCT of Fe–Cl complexes instead of additional HAT catalysts. Years ago, photooxidation and oxy-chlorination of cyclohexane in homogeneous phase were realised with this strategy,[14c–e] but the functionalisation type and substrate scope were quite limited. Very recently, Rovis Research Group successfully realised C(sp^3)–H bond alkylation *via* copper[14g] and iron[14h] photocatalysis with great substrate scope. However, direct C–H activation of gaseous alkanes with a similar chlorine-radical-mediated gaseous-liquid system met great difficulty due to their low solubility in most solvents and the little bond dissociation energy (BDE) difference between gaseous alkanes (such as ethane, 101.1 kcal mol^{-1})[15] and hydrogen chloride (103 kcal mol^{-1}).[15] Therefore, developing a concise and efficient system—that can transform C(sp^3)–H bonds, particularly of ethane and other gaseous alkanes, to diverse high value-added compounds under ambient temperature with high catalytic efficiency, low cost, low-oxidizability catalyst, and the convenience of being purified and scaled up—remains significantly challenging to scientists. As part of our continuing development on the photo-induced synthetic reactions,[16] we report here an extremely simple and highly efficient photo-induced catalytic system for selective C–H functionalisation of ethane, propane, and other light alkanes with the only-added iron catalyst (as cheap as \$USD 12 kg^{-1}) (Scheme 1). Many desired coupling products were obtained by a simple aqueous wash without chromatography; the reactions were consequently reliably scaled up and conveniently purified.

Results and discussion

First, the direct C–H transformation of cyclohexane (**1d**, a typical example of alkanes) to C–N bond was chosen as the model to investigate the iron-catalysed photoredox system. Table 1 shows several Fe(III) and Fe(II) salts screened with CH_3CN as the solvent under N_2 atmosphere and irradiation of 30 W 365 nm LED (entries 1–5). Only iron salts with chloride ions as anions could catalyse the C(sp^3)–H activation reaction and provide remarkable results (entries 3 and 4). To further investigate this phenomenon, extra chloride ions (tetraethylammonium chloride, TEAC) were added into the unreacted systems (entries 2 and 5). The result systems became effective for the model reaction (entries 6 and 7) in which the catalytic activity of Fe(III) seemed to be a little higher than Fe(II). The removal of iron ions will terminate the catalytic activities (entry 8) emphasising the need for both iron and chloride ions. Other metal chlorides and iron halides were also tried and no better results were observed (entries 9–12). The solvent in entry 3 was removed to confirm whether trace amount of other transition metals, especially noble metals with high activities of photocatalysis, catalysed this reaction instead of iron. The ICP mass spectrometry of the residue proved the low

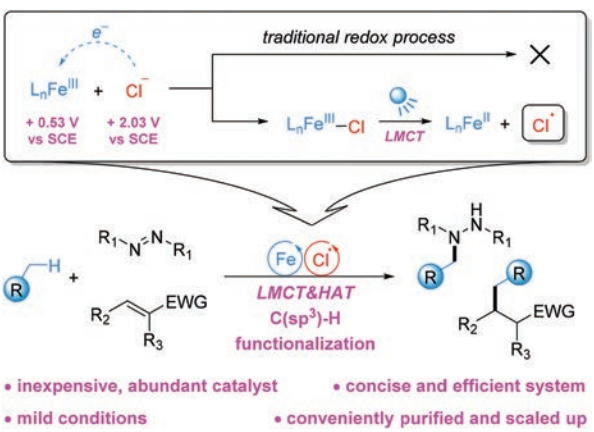

Scheme 1 Photo-induced C(sp^3)–H functionalisation *via* iron-catalysed LMCT/HAT processes. SCE = Saturated calomel electrode, EWG = electron withdrawing group.

Table 1 Optimisation of conditions for photo-induced Fe-catalysed C–N bond formation between cyclohexane (**1d**) and DBAD (**2a**)[a]

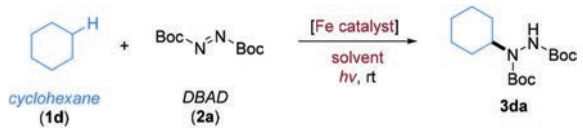

Entry	Fe catalyst	Solvent	Time (h)	Yield[b] (%)
1	$Fe_2(SO_4)_3{\cdot}H_2O$	CH_3CN	5.0	0
2	$Fe(NO_3)_3{\cdot}9H_2O$	CH_3CN	5.0	0
3	**$FeCl_3{\cdot}6H_2O$**	**CH_3CN**	**1.0**	**97**
4	Anhydrous $FeCl_2$	CH_3CN	1.0	94
5	$FeSO_4{\cdot}7H_2O$	CH_3CN	5.0	0
6	$Fe(NO_3)_3{\cdot}9H_2O$ + TEAC	CH_3CN	1.0	96
7	$FeSO_4{\cdot}7H_2O$ + TEAC	CH_3CN	1.0	46
8	TEAC	CH_3CN	5.0	Trace
9	$CuCl_2$	CH_3CN	1.0	28
10	$MnCl_2{\cdot}4H_2O$	CH_3CN	1.0	Trace
11	$NiCl_2$	CH_3CN	1.0	Trace
12	$FeBr_3$	CH_3CN	1.0	Trace
13[c]	—	CH_3CN	1.0	5.5
14	$FeCl_3{\cdot}6H_2O$	DMSO	1.0	0
15	$FeCl_3{\cdot}6H_2O$	CH_2Cl_2	1.0	25
16	$FeCl_3{\cdot}6H_2O$ (0.001 equiv.) + TEAC	CH_3CN	4.0	95
17	$FeCl_3{\cdot}6H_2O$ (0.0001 equiv.) + TEAC	CH_3CN	10.0	80 (TON = 8000)
18[d]	$FeCl_3{\cdot}6H_2O$	CH_3CN	5.0	0
19[e]	$FeCl_3{\cdot}6H_2O$	CH_3CN	5.0	56
20[f]	$FeCl_3{\cdot}6H_2O$	CH_3CN	5.0	17

[a] Reaction conditions: N_2 atmosphere and irradiation with 30 W 365 nm LED, cyclohexane (**1d**) (5 mmol, 10 equiv.), DBAD (**2a**) (0.5 mmol, 1 equiv.), Fe catalyst (5 μmol, 0.01 equiv.), additive (TEAC, 15 μmol, 0.03 equiv. if needed) solvent (5 mL), temperature (rt, ~25 °C), time (1–10 h) in a 10 mL quartz tube. [b] Yields of **3da** were determined by ^1H NMR using dibromomethane as the internal standard. [c] Cl_2 atmosphere. [d] No light. [e] Irradiation with 30 W 395 nm LED. [f] Irradiation with 30 W 405 nm LED. DBAD = ditertbutyl azodicarboxylate. TEAC = tetraethylammonium chloride. DMSO = dimethyl sulfoxide. TON = turnover number.

enough concentration of other transition metals.[17] Cl_2 atmosphere instead of iron catalysts under N_2 atmosphere was also tried, obtaining a somewhat messy system and a low yield of target product (entry 13, Fig. S21†). Next, the effect of the solvents was explored. Here, CH_3CN had the highest yield (compare entries 3, 14, 15). To survey the catalytic efficiency of iron catalyst, the catalyst loading was lowered to 0.001 equiv. (entry 16) and even 0.0001 equiv. (entry 17) resulting in longer reaction times and slightly decreased yields; the turnover number (TON) could be up to 8000. The reaction could not proceed without light irradiation (entry 18) and longer wavelengths reduced the yields of desired C–N bond formation product (entries 19 and 20). Importantly, the water-soluble ferric trichloride hexahydrate catalyst was the only additive inside the catalytic system except for the two substrates; the conversion rate of substrates to products was high enough, and thus a simple aqueous wash after reaction finishing produced the desired pure Boc-protected alkylhydrazine.

The Boc-protected alkylhydrazine is a valuable building block with economic and practical value.[11a,18] The substrate scope for the iron-catalysed photoredox C–H functionalisation of alkanes was surveyed with the optimised C–N bond formation conditions (Table 2). First, many familiar liquid and solid alkanes were attempted as substrates, and the corresponding C–N bond formation products (see **3da–3ia**) with ditertbutyl azodicarboxylate (DBAD) as radical trap were obtained in good to excellent yields. The regiomeric ratios (rr) of functionalisation products at different positions of alkanes were also investigated, and the results (such as 1 : 1.8 : 1 for **3fa**, 1.8 : 1.7 : 1 for **3ga**) showed that the regioselectivities depended on stabilities of the corresponding generated carbon radicals (3°/2°/1°) and quantities of hydrogens with a same chemical environment.[18d] Later calculations showed that the HAT regioselectivity (rs) among one 3°, 2°, and 1° hydrogen of alkanes in this catalytic system was close to 6 : 3 : 1;[18d] thus, the real regiomeric ratio among $H_1(2°) : H_2(2°) : H_3(1°)$ of **3fa** (1 : 1.8 : 1) was close to $(3 \times 2) : (3 \times 4) : (1 \times 6) = 1 : 2 : 1$. Different types of radical traps were also applied, and both C–N (see **3da–3dd**) and C–C bond formation (see **3de–3dp**) with alkanes provides good to excellent reaction efficiency.

Fixing natural gaseous alkanes and transforming them into valuable fine chemicals is a fundamentally intriguing challenge in organic synthesis.[19] This emphasises the benefits and importance of this approach. Here, *n*-butane is a major component of liquid petroleum gas (LPG). It offered an excellent yield under standard conditions and ambient pressure (see **3ca**). Meanwhile, the regioselective properties were similar to the values discussed above. Propane—the other major component of LPG—was then used as a substrate with a slightly lower yield of C–N bond formation product than that of butane due to the decreasing solubility in acetonitrile (see **3ba**). Another strong radical trap **2h** was applied and provided a more satisfactory result (see **3bh**). Ethane functionalisation is an enormous challenge according to the tiny solubility under ambient temperature and pressure. Lowering the concentration of the reaction, that means increasing the relative concentration of ethane, was an effective solution to promote the reaction yield (see Table S5†). We also employed different traps (see **3aa**, **3ab**, and **3ah**), and **2h** exhibited the best reactivity (see **3ah**).

Although various organic compounds with $C(sp^3)$–H bonds have been successfully functionalised by other groups,[7–13] trying these compounds with the practical catalytic method remains a tool to expand the substrate scope and, importantly, further investigate the regioselective properties of HAT processes. Table 2 shows that alkyl $C(sp^3)$–H bonds assembled with diverse functional groups, including arene (see **3ja**), ether (see **3ka–3na**, **3vh**), thioether (see **3qh**), ketone (see **3oa**), amide (see **3pa**), heteroarene (see **3th**), aliphatic (see **3rh**), and aromatic halogens (see **3sh**, **3uh**), can also be efficiently functionalised by photo-induced iron catalysis under standard conditions. Moreover, introduction of functional groups results in marked differences on the stabilities of HAT-generated radicals[6] such as the enhanced radical stabilities at alpha position of oxygen and nitrogen atoms (see **3ka–3na**, **3pa**), and the attenuated radical stabilities at the alpha position of ketone carbonyl (see **3oa**). This led to the different regiomeric ratios of each product. A low yield of **3ja**, **3sh** and **3uh** was obtained due to the well-known stability and dimerisation of the benzyl radical.[20] Another reason for affording unidentified by-products may be due to electrophilic reaction between intermediate chlorine radicals and arenes.[21] It should be mentioned that, for most gaseous (see **1a–1c**) and liquid alkanes (see **1d–1g**), the high enough yields and convenience of removing excess alkane substrates afford the purification of desired products without chromatography (see **3ah**, **3bh**, **3ca–3ga**, **3db–3dd**, **3dh–3do**). However, this strategy is always not suitable for substrates with functional groups due to their high boiling points and increase of by-products.

Whether a synthetic reaction can be conveniently scaled up and purified is a key factor to evaluate the synthetic practicability of the system. To demonstrate the outstanding practicability of the present Fe-catalysed photoredox $C(sp^3)$–H functionalisation protocol, a 10 mmol-scale synthesis with *n*-butane and a 50 mmol-scale synthesis with cyclohexane were performed (Scheme 2). After the reactions were completed, a simple aqueous wash toward the reaction mixture yielded 2.53 g of **3ca** in 87.8% yield and 14.79 g of **3da** in 94.1% yield without obvious loss of efficiency (more details see Fig. S3–S7†). It should be mentioned that although excess alkane substrates were added, little amount of them transformed to other by-products depending on GC analysis after reaction (Fig. S22†). Both excess liquid and gaseous alkane substrates could be recycled by after treatment for the next reaction.

Depending on the inspiration of previous work,[14e,h] some mechanistic experiments were performed to explore the mechanism of the photoredox $C(sp^3)$–H functionalisation systematically. Firstly, UV-visible absorption studies showed the coexistence of Fe^{3+} and Cl^- was responsible for the characteristic absorption peak near 365 nm, consistent with the data reported previously[14e,h] (more details see Fig. S14†). No similar

Table 2 Substrate scope for the photo-induced Fe-catalysed C(sp^3)–H functionalisation[a]

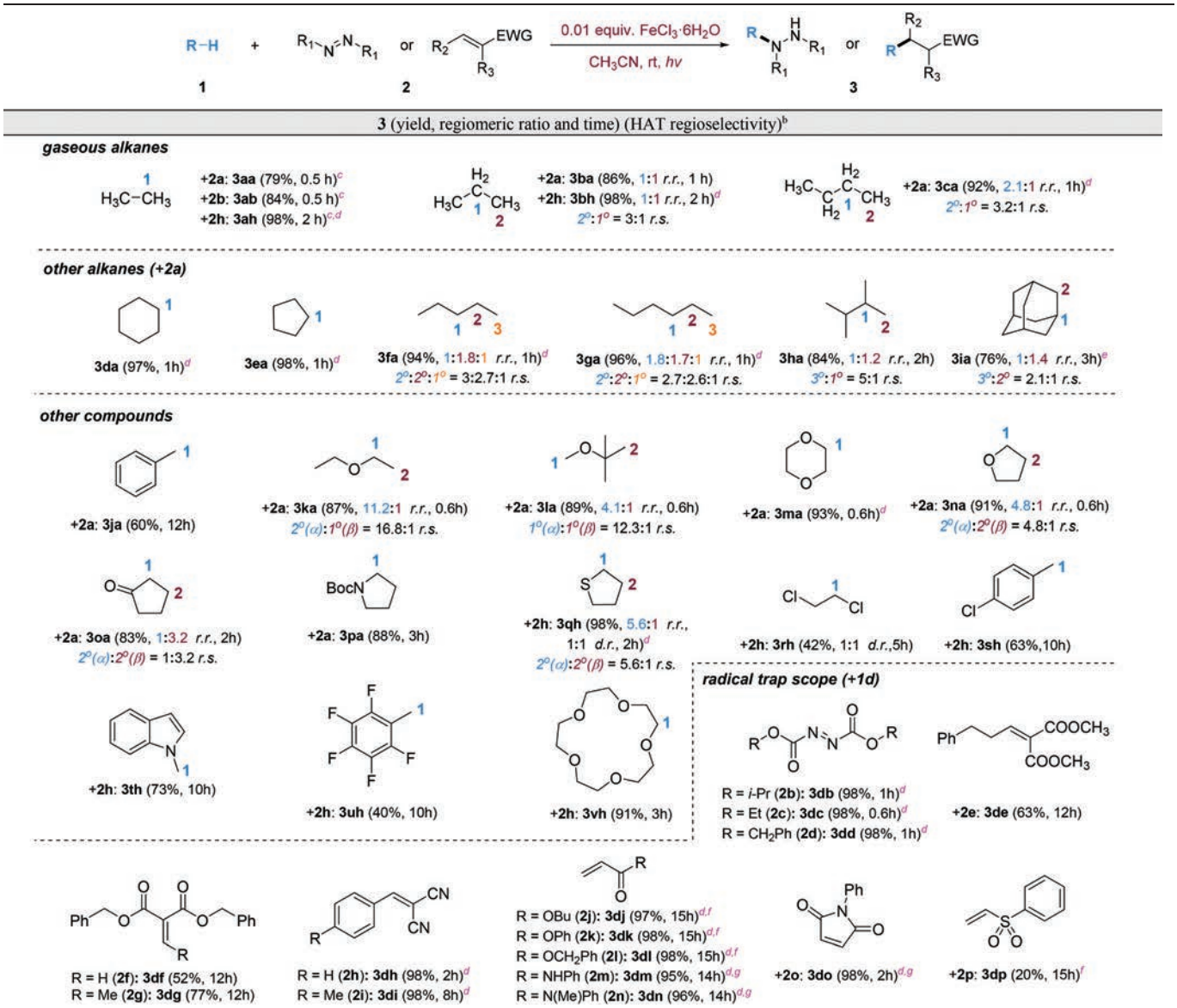

[a] Reaction conditions: N_2 atmosphere and irradiation with 30 W 365 nm LED, alkanes (**1**) (5 mmol, 10 equiv.), radical trap (**2**) (0.5 mmol, 1 equiv.), $FeCl_3{\cdot}6H_2O$ (5 μmol, 0.01 equiv.), CH_3CN (5 mL), temperature (rt, ~25 °C), time (0.5–12 h) in a 10 mL quartz tube. [b] Yields of **3** were determined by ^1H NMR analysis with internal standard; regiomeric ratios (rr) of **3** were determined by GC analysis; diastereo ratios (dr) were determined by GC/^1H NMR analysis; HAT regioselectivities (rs) were calculated by (regiomeric ratio)/(number of hydrogen). [c] The reaction was performed in 0.1 mmol scale with 0.03 equiv. catalyst and 7 mL CH_3CN. [d] The pure products can be obtained by aqueous wash without chromatography. [e] Regiomeric ratios (rr) were determined by ^1H NMR analysis. [f] The reaction was performed with 0.2 equiv. catalyst. [g] The reaction was performed with 0.1 equiv. catalyst.

absorption peak was found in UV-visible spectrum of pure $FeCl_2$ (see Fig. S15†). Time tracking of UV-visible spectrum reflected the obvious decomposition of $FeCl_3{\cdot}6H_2O$ under 365 nm LED irradiation (see Fig. S16†). Next, Stern–Volmer fluorescence quenching experiments were carried out. Among the components existing in the catalytic system, only Cl^- could quench the fluorescence of Fe^{3+} excited at 421 nm (see Fig. S17–S20†). This indicated a LMCT process instead of a traditional redox process between Fe^{3+} and Cl^-. The density of functional theory (DFT) calculation results also proved the LMCT process to take place according to the thermodynamic law (more details see Table S6†). Next, the radicals produced in the iron-catalysed system were surveyed by electron paramagnetic resonance (EPR) in the presence of 5,5-dimethyl-1-pyrroline *N*-oxide (DMPO) as the spin trapping agent. The EPR spectrum of mixture of $FeCl_3{\cdot}6H_2O$ (40 mM), cyclohexane (1 M), and DMPO (200 mM) in CH_3CN under dark condition showed no signal of trapped radicals. After irradiation for 60 s, the EPR spectrum became a combination of a triplet-signal (a_N = 1.496 mT, g = 2.0035) and a sextet-signal (a_N = 1.436 mT, a_H =

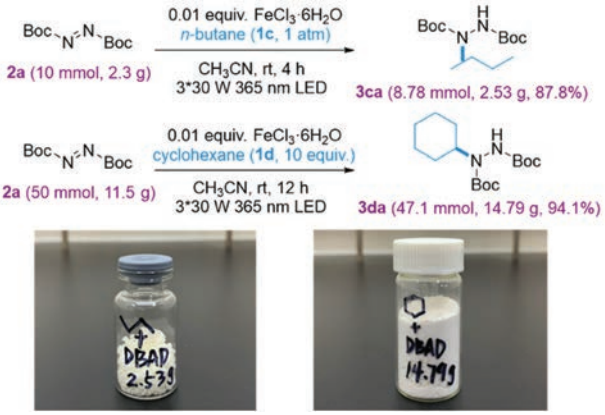

Scheme 2 Gram-scale synthesis of **3ca** and **3da**.

1.733 mT, g = 2.0039). The results indicated the appearance of chlorine and carbon radicals trapped by DMPO[22] (more details see Fig. S8–9†). The radical trapping experiments with 2,2,6,6-tetramethylpiperidine-1-oxyl (TEMPO) also demonstrated the appearance of carbon radicals generated from alkanes with ^{1}H NMR and GC-MS analysis (see Fig. S10–11†). To further study the photo-induced radical-intermediated system, the quantum yields (QY) of the reaction systems generating **3da** and **3dh** were 0.211 and 0.070 (see Fig. S12–13, Scheme S2–3†). This showed that radical chain processes made little contribution to generate the target C–N and C–C bond formation products.[23] The kinetic isotope effect (KIE) was evaluated by applying (a) cyclohexane/d_{12}-cyclohexane respectively as substrates or (b) a 1 : 1 mixture of cyclohexane and d_{12}-cyclohexane as substrates to produce **3da**. The magnitude of the KIE value given by k_H/k_D[24] and P_H/P_D[24] was 0.98 and 1.53 respectively for C–N bond formation (see Scheme S1†). These values indicated a chlorine-radical-intermediated HAT process to be a "product-determining step", but not the "rate-determining step" in this catalytic system.[24]

The above results suggest a possible mechanism for the iron-catalysed photoredox C(sp^3)–H functionalisation (Scheme 3).

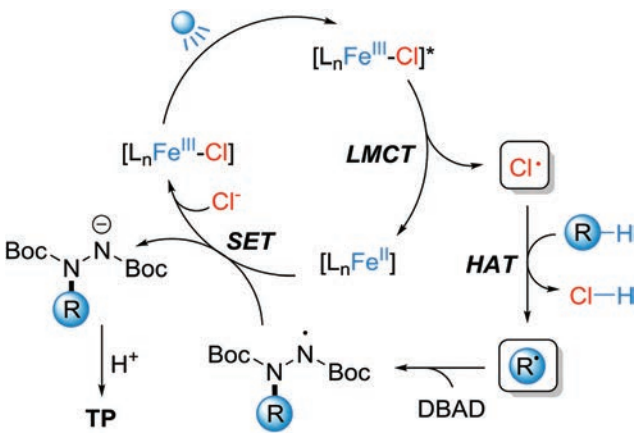

Scheme 3 Proposed mechanism for the iron-catalysed photoredox C–N bond formation between alkanes and DBAD. TP = Target product.

First, the Fe(III)–Cl complex transforms into its excited state under light irradiation. A subsequent LMCT provides an intermediate Fe(II) complex and a highly active chlorine radical. Next, a HAT process between the chlorine radical and C(sp^3)–H bond of alkane generates the corresponding alkyl radical and HCl. The alkyl radical is trapped by radical trap DBAD (chosen as an example) generating a new nitrogen radical. Sequentially, a single electron transfer (SET) occurs between the nitrogen radical and intermediate Fe(II) complex affording the final C–N bond effectively accelerated thanks to the high reducibility and coordination ability of Fe(II) intermediate compared to other catalytic systems.

Conclusions

We developed a highly efficient, green, and concise system for C(sp^3)–H functionalisation by iron photocatalysis. Alkanes including gaseous ethane, propane, and butane, as well as compounds with diverse functional groups, can be activated through this method by chlorine radicals generated from Fe(III)–Cl LMCT processes. It is a rare example of realising gaseous alkane functionalisation in gaseous-liquid phases with a chlorine radical-mediated process. This method exhibits many significant advantages including mild conditions, high reaction efficiency, low cost, and convenience of purification and amplification. We believe that this sustainable, convenient and environmentally friendly system will find wide applications in high value-added transformation of natural alkanes and offer novel inspiration for not only organic synthesis, but also design of catalytically active organic/inorganic materials (such as metal–organic frameworks, and zeolites).

Conflicts of interest

There are no conflicts to declare.

Acknowledgements

The authors would like to thank Dr Min Wang in this department for his great helps in analysis of gas chromatography, Dr Haijun Yang at Tsinghua University for his great helps in analysis of electron paramagnetic resonance, and Dr Haifang Li at Tsinghua University for her great helps in analysis of high resolution mass spectrometry. We acknowledge the support of the National Natural Science Foundation of China (21901032, 21890381, 21531001) and the Fundamental Research Funds for the Central Universities (DUT21LK13).

Notes and references

1 U.S. Energy Information Administration, International Energy Outlook 2019; https://www.eia.gov/outlooks/ieo/pdf/ieo2019.pdf.

2 (*a*) N. Gunsalus, J. A. Koppaka, S. H. Park, S. M. Bischof, B. G. Hashiguchi and R. A. Periana, *Chem. Rev.*, 2017, **117**, 8521; (*b*) A. E. Shilov and G. B. Shul'pin, *Chem. Rev.*, 1997, **97**, 2879; (*c*) R. A. Periana, D. J. Taube, S. Gamble, H. Taube, T. Satoh and H. Fujii, *Science*, 1998, **280**, 560; (*d*) R. A. Periana, O. Mironov, D. Taube, G. Bhalla and C. J. Jones, *Science*, 2003, **301**, 814; (*e*) M. V. Kirillova, M. L. Kuznetsov, P. M. Reis, J. A. L. da Silva, J. J. R. F. da Silva and A. J. L. Pombeiro, *J. Am. Chem. Soc.*, 2007, **129**, 10531; (*f*) A. Caballero, E. Despagnet-Ayoub, M. M. Díaz-Requejo, A. Díaz-Rodríguez, M. E. González-Núñez, R. Mello, B. K. Muñoz, W.-S. Ojo, G. Asensio, M. Etienne and J. P. Pérez, *Science*, 2011, **332**, 835.

3 R. H. Crabtree, *Chem. Rev.*, 1995, **95**, 987.

4 (*a*) V. N. Cavaliere, B. F. Wicker and D. J. Mindiola, *Adv. Organomet. Chem.*, 2012, **60**, 1; (*b*) K. T. Smith, S. Berritt, M. González-Moreiras, S. Ahn, M. R. Smith, 3rd, M.-H. Baik and D. J. Mindiola, *Science*, 2016, **351**, 1424; (*c*) A. K. Cook, S. D. Schimler, A. J. Matzger and M. S. Sanford, *Science*, 2016, **351**, 1421.

5 (*a*) X. Huang and J. T. Groves, *J. Biol. Inorg. Chem.*, 2017, **22**, 185; (*b*) Y. Liu, T. You, H.-X. Wang, Z. Tang, C.-Y. Zhou and C.-M. Che, *Chem. Soc. Rev.*, 2020, **49**, 5310.

6 (*a*) C. R. J. Stephenson, T. P. Yoon and D. W. C. MacMillan, *Visible Light Photocatalysis in Organic Chemistry*, Wiley, 2019; (*b*) K. L. Skubi, T. R. Blum and T. P. Yoon, *Chem. Rev.*, 2016, **116**, 10035; (*c*) N. A. Romero and D. A. Nicewicz, *Chem. Rev.*, 2016, **116**, 10075.

7 (*a*) S. Mukherjee, B. Maji, A. Tlahuext-Aca and F. Glorius, *J. Am. Chem. Soc.*, 2016, **138**, 16200; (*b*) K. A. Margrey, W. L. Czaplyski, D. A. Nicewicz and E. J. Alexanian, *J. Am. Chem. Soc.*, 2018, **140**, 4213; (*c*) J. Yu, C. Zhao, R. Zhou, W. Gao, S. Wang, K. Liu, S.-Y. Chen, K. Hu, L. Mei, L. Yuan, Z. Chai, H. Hu and W. Shi, *Chem. – Eur. J.*, 2020, **26**, 16521; (*d*) C. Huang, J.-H. Wang, J. Qiao, X.-W. Fan, B. Chen, C.-H. Tung and L.-Z. Wu, *J. Org. Chem.*, 2019, **84**, 12904; (*e*) D. Xia, Y. Li, T. Miao, P. Li and L. Wang, *Green Chem.*, 2017, **19**, 1732; (*f*) S. Paul and J. Guin, *Green Chem.*, 2017, **19**, 2530.

8 (*a*) J. L. Jeffrey, J. A. Terrett and D. W. C. MacMillan, *Science*, 2015, **349**, 1532; (*b*) G. J. Choi, Q. Zhu, D. C. Miller, C. J. Gu and R. R. Knowles, *Nature*, 2016, **539**, 268; (*c*) J. C. K. Chu and T. Rovis, *Nature*, 2016, **539**, 272; (*d*) C. Le, Y. Liang, R. W. Evans, X. Li and D. W. C. MacMillan, *Nature*, 2017, **547**, 79; (*e*) X.–A. Liang, L. Niu, S. Wang, J. Liu and A. Lei, *Org. Lett.*, 2019, **21**, 2441.

9 J. D. Cuthbertson and D. W. C. MacMillan, *Nature*, 2015, **519**, 74.

10 (*a*) D. R. Heitz, J. C. Tellis and G. A. Molander, *J. Am. Chem. Soc.*, 2016, **138**, 12715; (*b*) P. Jia, Q. Li, W. C. Poh, H. Jiang, H. Liu, H. Deng and J. Wu, *Chem*, 2020, **6**, 1766.

11 (*a*) A. Hu, J.-J. Guo, H. Pan and Z. Zuo, *Science*, 2018, **361**, 668; (*b*) H.-P. Deng, Q. Zhou and J. Wu, *Angew. Chem., Int. Ed.*, 2018, **57**, 12661; (*c*) G. Laudadio, Y. Deng, K. van der Wal, D. Ravelli, M. Nuño, M. Fagnoni, D. Guthrie, Y. Sun and T. Noël, *Science*, 2020, **369**, 92.

12 (*a*) S. Rohe, A. O. Morris, T. McCallum and L. Barriault, *Angew. Chem., Int. Ed.*, 2018, **57**, 15664; (*b*) M. Zidan, A. O. Morris, T. McCallum and L. Barriault, *Eur. J. Org. Chem.*, 2020, 1453; (*c*) W. Liu, X. Yang, Z.-Z. Zhou and C.-J. Li, *Chem*, 2017, **2**, 688.

13 B. J. Shields and A. G. Doyle, *J. Am. Chem. Soc.*, 2016, **138**, 12719.

14 (*a*) S. Xia, K. Hu, C. Lei and J. Jin, *Org. Lett.*, 2020, **22**, 1385; (*b*) Z. Li, X. Wang, S. Xia and J. Jin, *Org. Lett.*, 2019, **21**, 4259; (*c*) G. B. Shul'pin and M. M. Kats, *React. Kinet. Catal. Lett.*, 1990, **41**, 239; (*d*) G. B. Shul'pin, G. V. Nizova and Y. N. Kozlov, *New J. Chem.*, 1996, **20**, 1243; (*e*) W. Wu, Z. Fu, X. Wen, Y. Wang, S. Zou, Y. Meng, Y. Liu, S. R. Kirk and D. Yin, *Appl. Catal., A*, 2014, **469**, 483; (*f*) Z.-Y. Tan, K.-X. Wu, L.-S. Huang, R.-S. Wu, Z.-Y. Du and D.-Z. Xu, *Green Chem.*, 2020, **22**, 332; (*g*) S. M. Treacy and T. Rovis, *J. Am. Chem. Soc.*, 2021, **143**, 2729; (*h*) Y. C. Kang, S. M. Treacy and T. Rovis, *ACS Catal.*, 2021, **11**, 7442.

15 Y.-R. Luo, *Comprehensive Handbook of Chemical Bond Energies*, CRS, Florida, 2007.

16 (*a*) Y. Jin, L. Ou, H. Yang and H. Fu, *J. Am. Chem. Soc.*, 2017, **139**, 14237; (*b*) Y. Jin, H. Yang and H. Fu, *Chem. Commun.*, 2016, **52**, 12909; (*c*) Y. Jin, H. Yang and H. Fu, *Org. Lett.*, 2016, **18**, 6400; (*d*) Y. Jin, M. Jiang, H. Wang and H. Fu, *Sci. Rep.*, 2016, **6**, 20068; (*e*) Y. Jin, Q. Zhang, Y. Zhang and C. Duan, *Chem. Soc. Rev.*, 2020, **49**, 5561; (*f*) Y. Jin and H. Fu, *Asian J. Org. Chem.*, 2017, **6**, 368; (*g*) T. Zhang, Y. Jin, Y. Shi, M. Li, J. Li and C. Duan, *Coord. Chem. Rev.*, 2019, **380**, 201.

17 Data determined by ICP mass spectrometry (molar concentration): Co = 0.031 ppm, Ni = 0.24 ppm, Cu = 0.21 ppm, Mn = 2.61 ppm, Pd = 0.048 ppm, Ru = 0.009 ppm, Rh = 0.58 ppb, Ir = 0.0077 ppm, Ce = 0.077 ppm.

18 (*a*) G.-Z. Wang, D.-G. Liu, M.-T. Liu and Y. Fu, *Green Chem.*, 2021, DOI: 10.1039/d1gc01210j; (*b*) W. Szymanski, J. M. Beierle, H. A. V. Kistemaker, W. A. Velema and B. L. Feringa, *Chem. Rev.*, 2013, **113**, 6114; (*c*) W.-C. Xu, S. Sun and S. Wu, *Angew. Chem., Int. Ed.*, 2019, **58**, 9712; (*d*) For rr comparison with other HAT reagents, see: Q. An, Z. Wang, Y. Chen, X. Wang, K. Zhang, H. Pan, W. Liu and Z. Zuo, *J. Am. Chem. Soc.*, 2020, **142**, 6216.

19 (*a*) A. Caballero and P. J. Pérez, *Chem. Soc. Rev.*, 2013, **42**, 8809; (*b*) V. Vidal, A. Théolier, J. Thivolle-Cazat and J. Basset, *Science*, 1997, **276**, 99.

20 H. Qrareya, D. Ravelli, M. Fagnoni and A. Albini, *Adv. Synth. Catal.*, 2013, **355**, 2891.

21 K. Ohkubo, K. Mizushima and S. Fukuzumi, *Res. Chem. Intermed.*, 2013, **39**, 205.

22 (*a*) G. R. Buettner, *Free Radical Biol. Med.*, 1987, **3**, 259; (*b*) R. Song, H. Wang, M. Zhang, Y. Liu, X. Meng, S. Zhai, C.-C. Wang, T. Gong, Y. Wu, X. Jiang and W. Bu, *Angew. Chem., Int. Ed.*, 2020, **59**, 21032.

23 M. A. Cismesia and T. P. Yoon, *Chem. Sci.*, 2015, **6**, 5426–5434.

24 E. M. Simmons and J. F. Hartwig, *Angew. Chem., Int. Ed.*, 2012, **51**, 3066.